Available online at www.sciencedirect.com
SCIENCE DIRECT®
Chemical Physics Letters 405 (2005) 252–257
CHEMICAL PHYSICS LETTERS
www.elsevier.com/locate/cplett

In situ formation of solid-supported lipid/DNA complexes

Giulio Caracciolo [a], Heinz Amenitsch [b], Claudia Sadun [a], Ruggero Caminiti [a,*]

[a] Department of Chemistry and INFM, University of Rome 'La Sapienza', p.le Aldo Moro 5, 00185 Rome, Italy
[b] Institute of Biophysics and X-ray Structure Research, Austrian Academy of Sciences, Schmiedelstrasse 6, A-8042 Graz, Austria

Received 28 December 2004; in final form 8 February 2005
Available online 9 March 2005

Abstract

Solid-supported lipid/DNA complexes were prepared by using highly aligned 1,2-dioleoyl-3-trimethylammonium-propane (DOTAP) multibilayers as a template. The complex formation was promoted in situ and followed in time. The resulting DOTAP/DNA complex shows a good degree of orientation along the normal to the support as revealed by combined time-resolved energy dispersive X-ray diffraction (EDXD) and surface synchrotron small angle X-ray scattering (SAXS) measurements.

1. Introduction

Gene therapy, because of its aim to eradicate causes rather than symptoms of diseases, is widely believed to be the therapy of the 21st century. Recent completion of the working draft of the human genome mapping has unquestionably reinforced the hope of using gene medicines to combat genetic diseases. Over the last several years, various viral and nonviral methods for gene delivery have been actively investigated.

When mixing aqueous solutions of DNA with a suspension of cationic liposomes, highly condensed self-assembled cationic lipid/DNA complexes, named lipoplexes, are formed with the negative charge carried by the phosphate groups of the DNA neutralized by the cationic lipids [1].

The present knowledge about the structural properties of lipoplexes has been recently reviewed [2,3, and references therein] and it is now well established that the lipoplex often consists of a multilamellar structure comprising a periodic one-dimensional lattice of parallel DNA strands confined between two-dimensional (2D) lipid bilayers (L_α^c phase). The driving force of lipoplexes self-assembly is the entropic gain in releasing the Manning condensed counterions both from the cationic lipids and the DNA. Nowadays, despite of the numerous studies both theoretical and experimental, cationic liposomes are generally developed on the basis of trial and error by using expression of the transgene as a tool to evaluate their efficiency. In spite of the advantages in the use of lipoplexes for gene delivery purposes, cytotoxicity and immunogenic response associated with the use of cationic lipids are the major drawbacks that limit their employment as possible gene delivery vectors. Recently, new formulations have also been experienced based on the exclusive use of neutral lipids which are completely not-cytotoxic. In these complexes, divalent cations (Mn^{2+}, Ca^{2+}, Co^{2+}, Mg^{2+}, Fe^{2+}) behave as cationic lipids condensing DNA and promoting the formation of stable ternary complexes in which the DNA is embedded between alternating lipid bilayers. The inner structure revealed by X-ray diffraction appears very similar to the lamellar liquid-crystalline L_α^c phase found in lipoplexes [4–6]. More recently, McManus et al. [8] reported for the first time the existence of a highly ordered rectangular columnar phase in DNA–Ca^{2+}–neutral lipid complex similar to that previously observed by Artzner et al. [9] in cationic lipid/DNA complexes. In this study, the central importance of very long time scale relax-

* Corresponding author. Fax: +3906490631.
E-mail address: r.caminiti@caspur.it (R. Caminiti).

0009-2614/$ - see front matter © 2005 Elsevier B.V. All rights reserved.
doi:10.1016/j.cplett.2005.02.047

ational process in ordering lipid/DNA complexes has been highlighted [7]. So, time-resolved experiments are expected to shed more light on the long time scale kinetics of lipid/DNA complexes.

On the other hand, because gene transfection involves the formation of discrete complexes, it is well recognized that the enhancement of transfection efficiencies via cationic lipids require a full understanding of all the possible supramolecular structures of lipoplexes at the molecular and self-assembled levels [2, and references therein].

Accordingly, accurate structural characterization of lipoplexes should help towards a deeper understanding of the mechanisms of transfection and of the mode by which the structure and size of cationic liposomes affect the physico-chemical properties and biological activity of the lipoplexes themselves. For gene delivery purposes, multi-lamellar vesicles (MLV) are widely utilized consisting of independent scattering domains each of which is a stack of parallel bilayers with the normals to the bilayers in independent stacks isotropically distributed in space. Such powder-like samples weakly diffract and the intensity rapidly falls off with increasing transfer momentum q. Conversely, solid-supported highly aligned lipid multilayers safeguard spatial information and give more intensity for higher orders of diffraction allowing for more accurate diffraction analyses. The major drawback of measuring oriented samples in humidity chambers has for a long time been the so-called vapour pressure paradox (VPP) whose theoretical background explained why aligned multibilayers hydrated from vapour usually exhibited reduced level of hydration [10]. Recently, Katsaras has demonstrated that VPP originated only from experimental inadequacy and has shown that aligned multibilayers can hydrate to the same extent as liposomes immersed in water [11]. As a result, the field of lipid bilayers structure research has started to use oriented stacks of bilayers hydrated from vapour as model systems of biological membranes [12].

In this Letter, we extended this approach to the in situ formation of solid-supported lipoplexes by using highly aligned stacks of membranes as a template. While the polymeric properties of DNA molecules bound to solid-supported cationic membranes have been recently investigated [13], to our knowledge, no previous experimental study has concerned the in situ formation of solid-supported lipoplexes. Kinetic experiments performed both by time-resolved energy dispersive X-ray diffraction (EDXD) and synchrotron small angle X-ray scattering (SAXS) allowed us to resolve the lipid/DNA complex formation in situ. Furthermore, we retrieved detailed information about the structure, the degree of order and the orientation of the emerging solid-supported lipoplexes, both dehydrated and fully hydrated from a vapour saturated atmosphere. By orientation, important new insight may be obtained into the structural organization of lipoplexes. For example, the lineshape analysis of high-resolution diffraction peaks from oriented samples is expected to clarify the short-ranged positional cross correlations between the DNA of adjacent layers whereas effects of powder-averaging can cause this cross correlations to vanish and not to be observed in unoriented samples. Thus, the use of oriented samples, could shed more light into the existence of the theoretically predicted 'new sliding columnar phase' of matter which has been supposed to exist in layered systems composed of weakly coupled 2D smectic lattices [14]. Such biomolecular templatings could also be relevant on the future development of practical device engineering of industrial interest.

2. Materials and methods

2.1. Sample preparation

A multilayered stack of highly aligned 1,2-dioleoyl-3-trimethylammonium-propane (DOTAP) membranes was prepared depositing 1 mg of DOTAP onto the $\langle 1\,0\,0\rangle$ oriented surface of a silicon wafer (area $\sim$ 1.5 cm^2) by evaporating from an isopropanol solution (10 mg/ml). DOTAP, which is an amphipatic cationic lipid consisting of 18-carbon (C_{18}) oleic acid chains esterified to a trimethylammonium moiety, was purchased from Avanti Polar Lipids in the lyophilized form and used without further purification. After drying under a vacuum over at least 12 h to remove any residual solvent, the sample was transferred to the X-ray chamber. An ultra pure water solution of double-stranded calf thymus DNA (MW(bp) = 649) 5.6 mg/ml was sonicated for 30 s. Since DNA carries two negative charges/bp whereas each DOTAP molecule has one positive charge head group, the complex is stoichiometrically neutral when the numbers of DNA bases and DOTAP molecules are equal and the lipid/DNA weight ratio $\rho = \rho^{iso} = 2 * MW(DOTAP)/MW(bp) = 2.2$.

2.2. EDXD experiments

X-ray diffraction experiments were carried out by using an EDXD apparatus elsewhere described [15]. The X-ray source is a standard Seifert tube operating at 50 kV and 40 mA whose Bremsstrahlung radiation is used, whereas the detecting system is composed of an EG&G liquid-nitrogen-cooled ultrapure Ge solid-state detector. The diffractometer, equipped with step motors and a collimating system, operates in vertical θ/θ geometry and both the X-ray tube and the detector can rotate around their common centre in which the lipid coated wafer is placed. The uncertainty associated to θ is $\Delta\theta = 0.001°$ and it directly affects the uncertainty Δq associated to the transfer momentum q ($q = \cos t * E * \sin\theta$; $\cos t = 1.01354\ \text{Å}^{-1} * \text{keV}^{-1}$). Each EDXD scan

was collected for a period of time $10 < t < 1000$ s, depending on the desired statistical accuracy. Biological samples are not damaged by EDXD experiments as elsewhere discussed [16]. Diffraction data were routinely corrected [15].

2.3. SAXS experiments

All SAXS measurements were performed at the Austrian SAXS station of the synchrotron light source ELETTRA (Trieste, Italy) [17]. For the measurements a surface diffraction cell has been utilized, which was specifically designed to perform in situ surface chemistry (for technical details see [18]). The photon energy was set to 8 keV. The ω-rotations of the specimen were performed with a high precision cradle (angular resolution: 0.001°; BGM 80 PP Goniometeric Cradle, Newport, De Saint Guenault, France). The diffraction patterns were recorded by a CCD-detector (Model CV 12, Photonic Science Ltd., Millham, UK). The beamline was set to resolve an angular regime from about 1/300 to 1/15 $Å^{-1}$, and silver behenate ($CH_3(CH_2)_{20}$-COOAg, d-spacing of 58.38 Å) was used as a standard to calibrate the angular dependence of the scattered intensity. All the SAXS images were corrected for electronic dark noise, spatial distortion and detector efficiency. This data reduction was performed with the software package FIT2D [19].

3. Results and discussion

The EDXD pattern of DOTAP multibilayers system is displayed in Fig. 1 as a function of perpendicular momentum transfer q_z. Four orders of sharp Bragg peaks (BPs) are recorded indicating a high degree of translational order along the normal to the lipid bilayer (z-direction) and a lamellar periodicity of $d = 2\pi/q = 48.0$ Å. This value strictly depends on the level of hydration of the sample as elsewhere extensively discussed [20]. The inset labeled as (a) shows a typical rocking curve at the first BP with a central full width at half maximum (FWHM) of 0.06°. From the diffraction pattern of Fig. 1, we also calculated the electron density profile along the normal to the DOTAP bilayers. Due to the bilayer nature of the molecular arrangement, the electron density has a centre of symmetry in the middle of the bilayer where the methyl groups stay. The electron density profile, $\Delta\rho$, along the normal to the bilayers, z, was then calculated as a Fourier sum of cosine terms

$$\Delta\rho = \frac{\rho(z) - \langle\rho\rangle}{\left[\langle\rho^2(z)\rangle - \langle\rho\rangle^2\right]^{1/2}} = \sum_{l=1}^{N} F_l \cos\left(2\pi l \frac{z}{d}\right), \qquad (1)$$

where $\rho(z)$ is the electron density, $\langle\rho\rangle$ its average value, N is the highest order of observed reflections, F_l is the form factor for the (0 0 l) reflection, d is the thickness of the repeating unit.

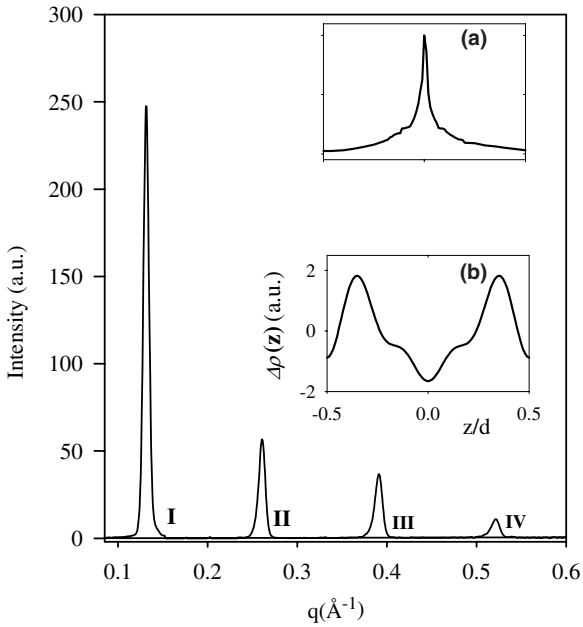

Fig. 1. EDXD pattern of pure DOTAP ($T = 300$ K, RH = 50%) shows four sharp Bragg reflections. A representative rocking scan measured at the first Bragg peak (panel (a)) proves the very good alignment of the DOTAP membranes. Electron-density profile along the normal to the bilayers in the L_α phase is also reported (panel (b)).

The discrete bilayer form factor is obtained from the integrated intensity $I_h = F_h^2/C_h$ under the hth diffraction peak, where C_h is the Lorentz-polarization correction factor. For a centrosymmetric and one-dimensional structure the form factor is a real number either positive or negative.

The choice of the best sign sequence for the structure factor, i.e., the phase problem, was solved using the approach originally proposed by Luzzati et al. [21]. The sign combination used to calculate the electron density profile is $--+-$ relative to the structures factors F_1, F_2, F_3, F_4 [22].

The calculated electron density profile over the unit cell of solid-supported DOTAP multilayer is reported in Fig. 1 (inset b) where the electron denser regions (i.e., the two maxima) correspond to the lipid headgroups while the large central minimum corresponds to the region of the hydrocarbon tails. The distance between the maxima of electron density is usually considered a good estimate of the bilayer thickness d_{HH} [21]. From the electron density profile reported in Fig. 1, the thickness of lipid bilayer $d_{HH} = 33.6$ Å was calculated. This value is in good agreement with that previously obtained for DOTAP liposomes in bulk [23]. Since the lamellar d-spacing is the sum of two structural components, i.e., the bilayer thickness, d_{HH}, and water-layer thickness, d_w, the interbilayer water thickness can be defined as $d_w = d - d_{HH}$. From this relation a water thickness $d_w = 14.4$ Å was also calculated.

A drop of 40 μl of a DNA solution 5.6 mg/ml was then carefully spread onto the solid/air interface of the lipid film at a lipid/DNA weight ratio $\rho = 4.1$, covered the overall surface of the lipid film and the solvent was let evaporate. To resolve the complex formation, time-resolved EDXD patterns were recorded due to the peculiar characteristics of EDXD which has recently appeared to be of great interest in studying the kinetic variation of ordered structures (lipid bilayer) induced by the change of physical and/or chemical parameters [24]. After the drop spreading, diffraction intensity was accumulated for 100 s per spectrum. In EDXD data collection, no mechanical movement is required, so that the restart of a new spectrum is simply a matter of storing and starting counting again. Even if a detailed kinetic study will be provided elsewhere, EDXD patterns representative of the temporal evolution of the system are reported in Fig. 2. To the sake of clarity, the top pattern ($t = 0$) represents the first-order DOTAP BP immediately before the drop spreading. At $t = 50$ s (Fig. 2) a single BP is visible at $q = 0.108$ Å^{-1} ($d = 58.2$ Å) which shifts to lower q-values as a function of time up to $t = 20\,000$ s ($d \sim 63.5$ Å). This finding can be interpreted in terms of DNA condensation between opposing DOTAP bilayers. During this period of time, DNA enters the lipid multilayer enlarging the thickness of the inter-bilayers water regions.

Upon further drying, a progressive shift to higher q-values of the BP occurs because the system starts to loose bulk water molecules between opposing bilayers in order to reach the thermodynamic equilibrium with the surrounding environment (relative humidity RH $\sim$ 45%). At $t = 25\,000$ s, the EDXD pattern clearly shows that the formed DOTAP/DNA complex starts to coexist with uncomplexed original DOTAP membranes as in the case of DOTAP/DNA unoriented lipoplexes [23]. At the final stage ($t = 35\,000$ s), the pure lipid BP intensity is less than a hundredth of its initial value confirming that the major part of DOTAP membranes is involved in the DOTAP/DNA complex formation.

After complete drying, the final EDXD pattern displayed in Fig. 3 (panel a) shows a sharp peak at $q = 0.113$ Å^{-1} corresponding to the (0 0 1) reflection of an ordered multilamellar structure with a periodicity $d \sim 55.7$ Å. Our experimental findings are clearly interpretable in terms of DNA condensation between lipid bilayers and are in excellent agreement with structural information previously obtained on unoriented dehydrated lipid/DNA complexes [25,26]. Therefore, the deposition of the DNA solution immediately resulted in the spontaneous self-assembly of cationic lipids and DNA fragments into the lamellar L_α^c liquid-crystalline phase. Upon complexation the cationic lipids effectively act as counterions neutralizing the negative charge of DNA [27]. From the above calculated thickness d_{HH}, we can conclude that the retrieved lamellar periodicity

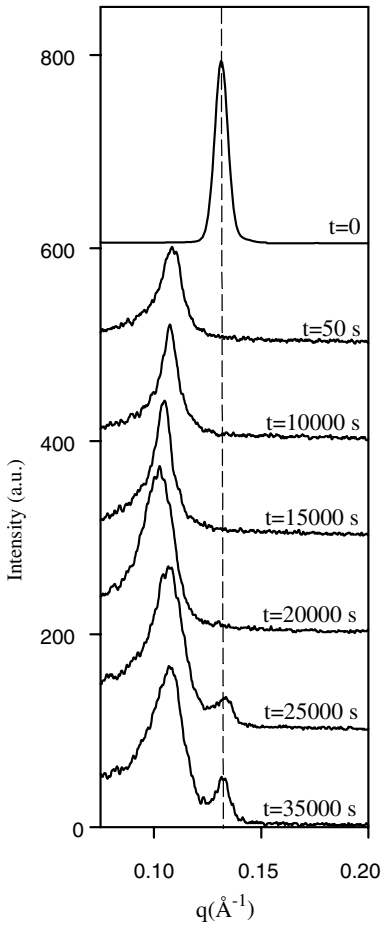

Fig. 2. Representative time-resolved EDXD patterns collected upon DOTAP–DNA complex formation as a function of time. The top pattern represents the first-order BP of pure DOTAP before the DNA solution spreading (to clarity intensity was divided by a factor 10). At $t = 35\,000$ s, the system is dehydrated and the EDXD pattern shows the presence of predominant DOTAP–DNA complex coexisting with a reduced amount of uncomplexed DOTAP membranes (dashed line).

is enough to accommodate the DNA molecules between two consecutive lipid bilayers. This result has confirmed the general expectation that the physical mechanisms underlying the lipoplex formation are the same even in the case of solid-supported samples, enforcing the idea of using them as model systems for the study of the structural properties of lipoplexes.

Before attempting to claim that the proposed experimental procedure effectively resulted in the formation of oriented lipoplexes, the degree of orientation in the samples was promptly investigated. To this end, rocking scans were taken at both the first-order BP of the complex and the lipid and are simultaneously displayed in the inset of Fig. 3 (panel a). The rocking scan proves the good alignment of the lipid/DNA complex with a mosaicity (FWHM = 0.1°) lower but comparable with that of the pure lipid system (FWHM = 0.06°). The higher FWHM value is due to the onset of stacking disorder induced by the DNA. This is an indication that the DNA fragments intercalate into the aqueous region

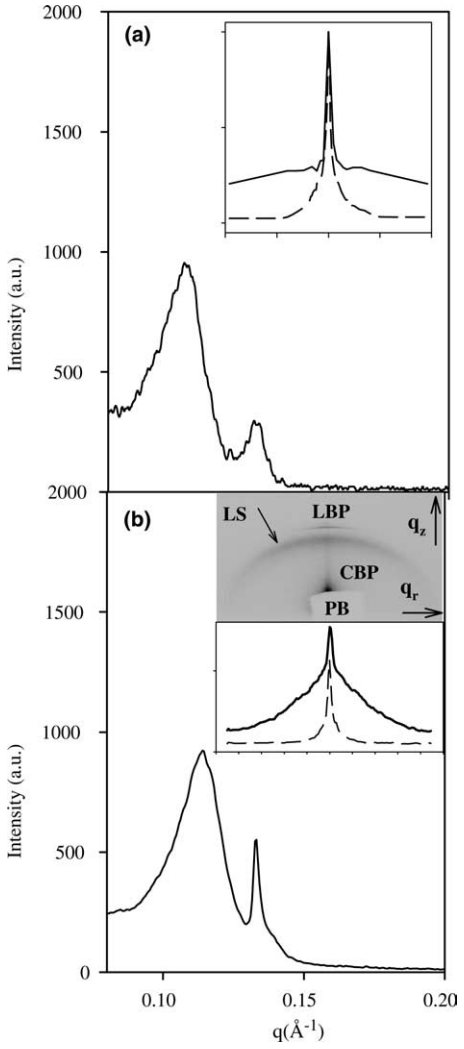

Fig. 3. EDXD pattern of dehydrated DOTAP–DNA complex plus DOTAP membranes (panel (a)). In the inset of panel (a), a direct comparison between the rocking scans measured at the first-order Bragg peak of the complex (solid line) and the pure lipid (dashed line) is reported. In the dehydrated state, the disorder in multilamellar DOTAP structure increases with DNA condensation. In the panel (b), a synchrotron X-ray pattern collected on the same system is shown. In the inset of panel (b), a 2D X-ray pattern (top) elucidates the orientation and of both the complex and the lipid. The first-order Bragg peak of the oriented complex (CBP) and that of the pure lipid (LBP) are evident even if unambiguous traces of liposomes-like structures (LS) are also present. The primary beam (PB) is also indicated. The curves (bottom) obtained by azimuthal integration (complex: solid line; pure lipid: dashed line) strictly confirm the EDXD results.

between opposing bilayers at the expense of uniformity of alignment. Conversely, the increase of diffuse scattering illustrates the simultaneous presence of liposome-like structures probably induced by hydrophobic interactions at the early stage of the complex formation. While a full discussion on the possible explanations behind this finding cannot be given here, it is only important to note that one can distinguish oriented (prevalent) and unoriented complexes. In order to shed more light on the degree of orientation of the emerging lipid/DNA complexes synchrotron SAXS measurements were also performed and a representative 2D X-ray pattern is displayed in Fig. 3, panel b. Two evident Bragg reflections, corresponding to d spacings of 57.1 and 48.5 Å, respectively, closely resemble those previously detected by EDXD experiments (Fig. 3, panel a). In addition, 2D X-ray pattern gives unambiguous information about the orientation of the lipoplexes formed in situ. While traces of the first-order BP of the pure lipid (BPL) remain, the SAXS pattern demonstrates that, upon spreading the DNA solution at the lipid/air interface, the DNA fragments penetrate into the major part of the aligned multilamellar DOTAP stacks. Even more remarkably, the pattern indicates that the arising multilamellar structure is preferentially oriented along the z-direction. However, subtle Debye–Scherrer rings due to traces of nonoriented liposomal scattering contributions (LS) are also detected.

EDXD and SAXS combined results suggest that the overall process can be simply schematized as displayed in Fig. 4. The excellent agreement between EDXD and SAXS results confirms that the proposed experimental procedure effectively resulted in the formation of solid-supported DOTAP/DNA complexes preferentially oriented along the normal to the support.

To extend all the retrieved structural information to the 'biologically relevant' full hydration condition, the solid-supported dehydrated sample was finally fully hydrated.

Closing the chamber windows, the dry film was fully hydrated from vapour until the repeat distance reached its limiting value ($d \sim 63.6$ Å). This full repeat distance is in a excellent accordance with that previously obtained in the case of unoriented DOTAP/DNA liposomes immersed in water [23].

The final EDXD pattern is reported in Fig. 5 together with a rocking curve at the first BP (panel a). The rock-

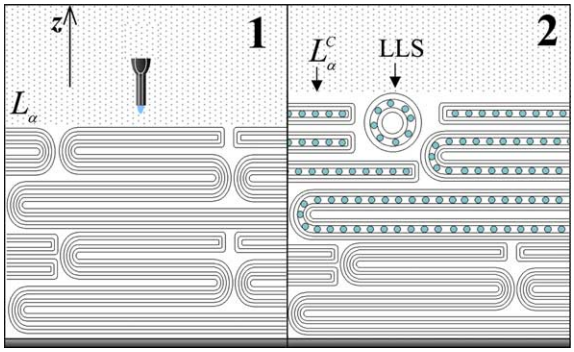

Fig. 4. Solid-supported aligned DOTAP multibilayers system in the liquid crystalline L_α phase (1). A drop of a DNA solution was spread at the lipid/air interface. This resulted in the spontaneous DNA condensation between opposing bilayers (L_α^c phase, 2). After excess solvent evaporation, the emerging DOTAP/DNA complex was found to coexist with liposome-likes structures (LLS). The DNA double helices are schematically represented by rods.

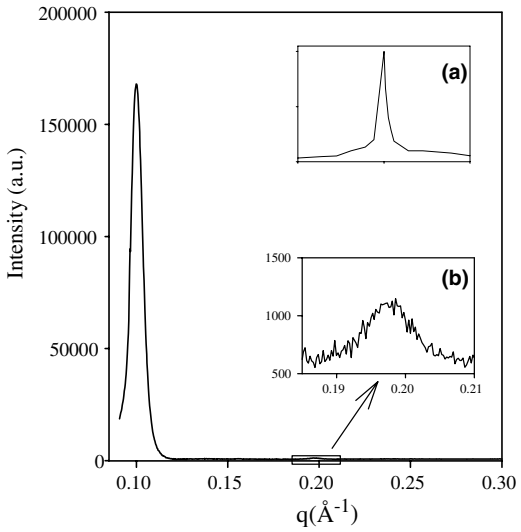

Fig. 5. EDXD pattern of DOTAP–DNA complex in the biologically significant full hydration condition. Two orders of a lamellar structure with a periodicity $d = 63.6$ Å are observed. The high alignment of the fully hydrated solid-supported complex is proved by a rocking scan collected at the first-order Bragg peak and reported in the panel (a). The second-order BP is shown in panel (b).

ing scan proves the high alignment of the fully hydrated lipid/DNA complex with the same mosaicity (FWHM = 0.06°) of the pure lipid system. Interestingly, we observe that, upon hydration, the lattice disorder decreases with respect to the dehydrated condition and the increase of spatial coherence leads to a progressive raise and sharpening of diffraction peaks. A possible explanation of this result is that the adsorbed water molecules can modulate the molecular arrangement of lipids with the headgroups locked into a highly ordered and stable structure as elsewhere proposed. Headgroup–headgroup interactions in the starting almost dry state could be replaced by stronger water-headgroups H bonds between water and lipid [28].

4. Conclusions

The proposed experimental procedure resulted in the formation of solid-supported lipid/DNA complexes with a sensible reduction of the typical EDXD acqui- sition times [23]. Our combined EDXD and SAXS results confirm that the inner structure of solid-supported complexes formed in situ is essentially the same as their counterpart in aqueous solution. As a result, solid-supported lipid/DNA complexes can successfully emerge as an interesting measurement condition in order to retrieve high-resolution structural information. The good degree of alignment obtained makes it also possible to apply advanced scattering techniques with a precise control of parallel and vertical components of the momentum transfer. Finally, the experimental set-up presented here is amenable to kinetic studies, where membrane active biomolecules solved in the excess water phase can interact with the bilayers. Aside from biomedical applications, since the details of the lipid and DNA molecular structure were not considered, we expect solid-supported DOTAP/DNA complexes to represent a model system and our findings to apply to a wide class of self-assemblies formed between several molecular components including proteins and/or peptides and membranes in their liquid-crystalline L_α state.

References

[1] P.L. Felgner, T.R. Gadek, M. Holm, R. Roman, H.W. Chan, M. Wenz, J.P. Northrop, G.M. Ringold, M. Danielsen, Proc. Natl. Acad. Sci. USA 84 (1987) 7413.
[2] C.R. Safinya, Curr. Opin. Struct. Biol. 11 (2001) 440.
[3] S. May, A. Ben-Shaul, Curr. Med. Chem. 11 (2004) 1241.
[4] J.J. McManus, J.O. Rädler, K.A. Dawson, J. Phys. Chem. B 107 (36) (2003) 9869.
[5] J.J. McManus, J.O. Rädler, K.A. Dawson, Langmuir 19 (23) (2003) 9630.
[6] G. Caracciolo, C. Sadun, R. Caminiti, M. Pisani, P. Bruni, O. Francescangeli, Chem. Phys. Lett. 397 (1–3) (2002) 138.
[7] O. Francescangeli, V. Stanic, L. Gobbi, P. Bruni, M. Iacussi, G. Tosi, S. Bernstorff, Phys. Rev. E 67 (2003) 011904.
[8] J.J. McManus, J.O. Rädler, K.A. Dawson, J. Am. Chem. Soc. 126 (2004) 15966.
[9] F. Artzner, R. Zantl, G. Rapp, J.O. Rädler, Phys. Rev. Lett. 81 (1998) 5015.
[10] R. Podgornik, V.A. Parsegian, Biophys. J. 72 (1997) 942.
[11] J. Katsaras, Biophys. J. 75 (1998) 2157.
[12] Y. Lyatskaya, Y. Liu, S. Tristram-Nagle, J. Katsaras, J.F. Nagle, Phys. Rev. E 63 (011097) (2001) 1.
[13] B. Maier, J.O. Rädler, Macromolecules 33 (2000) 7185.
[14] L. Golubovic, T.C. Lubensky, C.S. O'Hern, Phys. Rev. E 62 (2000) 1069.
[15] R. Caminiti, V. Rossi Alberini, Int. Rev. Phys. Chem. 18 (2) (1999) 263.
[16] G. Caracciolo, G. Amiconi, L. Bencivenni, G. Boumis, R. Caminiti, E. Finocchiaro, B. Maras, C. Paolinelli, A. Congiu Castellano, Eur. Biophys. J. 30 (2001) 163.
[17] H. Amenitsch, J. Appl. Crystallogr. 30 (1997) 872.
[18] H. Amenitsch, M. Rappolt, C.V. Teixeira, M. Majerowicz, P. Laggner, Langmuir 20 (2004) 4621.
[19] A.P. Hammersley, Rev. Sci. Inst. 66 (1995) 2729.
[20] G. Caracciolo, S. Sadun, R. Caminiti, Appl. Phys. Lett. 85 (9) (2004) 1630.
[21] V. Luzzati, P. Mariani, H. Delacroix, Makromol. Chem. Macromol. Symp. 15 (1998) 1.
[22] H.I. Petrache, S. Tristram-Nagle, K. Gawrisch, D. Harries, V.A. Parsegian, J.F. Nagle, Biophys. J. 86 (2004) 1574.
[23] G. Caracciolo, R. Caminiti, D. Pozzi, M. Friello, F. Boffi, A. Congiu Castellano, Chem. Phys. Lett. 351 (2002) 222.
[24] G. Caracciolo, G. Mancini, C. Bombelli, R. Caminiti, Chem. Phys. Lett. 386 (1–3) (2004) 76.
[25] G. Caracciolo, R. Caminiti, F. Natali, A. Congiu Castellano, Chem. Phys. Lett. 366 (2002).
[26] G. Caracciolo, D. Pozzi, R. Caminiti, A. Congiu Castellano, Eur. Phys. J. E 10 (2003) 331.
[27] R. Bruinsma, J. Mashl, Europhys. Lett. 41 (1998) 165.
[28] H. Binder, B. Kohlstrunk, W. Pohle, J. Phys. Chem. B 104 (2000) 12049.